Preparation and Physicochemical Characterization of Aqueous Dispersions of Coenzyme Q_{10} Nanoparticles

Britta Siekmann[1,2] and Kirsten Westesen[1,3]

Received February 11, 1994; accepted September 10, 1994

The present study describes a novel pharmaceutical formulation of coenzyme Q_{10}, viz. submicron-sized dispersions of the substance prepared by emulsification of molten coenzyme Q_{10} in an aqueous phase. Photon correlation spectroscopy reveals mean diameters of 60 to 300 nm depending on process parameters. Coenzyme Q_{10} nanoparticles remain stable on storage for more than 30 months. Lipophilic drugs can be incorporated into the nanoparticles demonstrating their potential use as a drug carrier system. Transmission electron micrographs of freeze-fractured replica show spherical particles with an amorphous core. Cryo-electron microscopy reveals the coexistence of small unilamellar vesicles in phospholipid stabilized dispersions. Thermoanalysis and X-ray studies indicate that the dispersed and emulsified coenzyme Q_{10} does not recrystallize even at 4°C over 30 months. These agree with ^{1}H NMR data which demonstrate that coenzyme Q_{10} molecules have a high mobility when formulated as nanoparticles and that colloidally dispersed coenzyme Q_{10} remains in the state of a supercooled melt. Despite the high melting point of the bulk material, coenzyme Q_{10} dispersions represent no suspensions but O/W emulsions according to the IUPAC definition (1).

KEY WORDS: coenzyme Q_{10}; drug nanoparticles; supercooled melt; physicochemical characterization; melt emulsification.

INTRODUCTION

Solid drug substances are commonly disintegrated by milling and grinding thereby generating particles in the millimeter and micrometer size range. A further decrease in size is expensive, ineffective or even impossible by conventional techniques. Moreover, ultrafine dry products are difficult to handle because of the risk of dust explosions, cross-contamination and inhalation of bioactive material. However, the particle size of drug compounds may have to be reduced below the micrometer size range.

Since the diameter of the smallest blood capillaries is only a few microns, intravenous (i.v.) administration of larger particles such as suspensions of water insoluble drugs would lead to capillary blockage. Moreover, particle size is one of the parameters governing the activity of the reticuloendothelial system (RES). In general, smaller particles are less rapidly cleared from the blood stream than larger ones (2).

Additionally, the bioavailability of perorally administered drugs is related to particle size via the dissolution rate, since in diffusion controlled dissolution of sparingly soluble suspended drugs the diffusional distance decreases substantially with particle size (3), and reduction in particle size leads to an increase in the interfacial surface area (4). In addition, colloidal particle dimensions result *inter alia* in an apparent change in equilibrium solubility as can be derived from the Gibbs-Kelvin equation (5).

The aim of the present study was to develop a simple and reproducible production method for submicron-sized drug particles. A reduction in particle size compared to conventional pharmaceutical formulations is supposed to enhance the bioavailability of perorally administered drugs, and furthermore enables the direct intravenous application of poorly water-soluble substances.

The endogenous quinone coenzyme Q_{10} (CoQ_{10}) which is therapeutically used *inter alia* for the treatment of heart diseases has been selected as a model drug. Due to the molecule's long side chain of 10 isoprenoid units, CoQ_{10} is extremely lipophilic and practically insoluble in water. The bioavailability of perorally administered CoQ_{10} is generally extremely low and was found to be related to the dissolution rate of the formulation (6). As a consequence of the low peroral bioavailability, intravenous administration systems are of special interest particularly in intensive care of heart attack patients. Due to its lipophilicity, CoQ_{10} needs to be incorporated into a carrier for i.v. administration so that its pharmacokinetics are influenced by the carrier system. Hence, CoQ_{10} accumulates in RES organs when administered intravenously as a mixed micellar system or in an emulsion vehicle, respectively (7).

Submicron-sized particles can be prepared from crystalline materials, e.g. glycerides, by emulsification of the molten compounds in an aqueous phase (8). Owing to the low melting point of CoQ_{10} which is 49°C (9), the same procedure could be applied to this drug substance. Thus, the object of the present study was to prepare CoQ_{10} nanoparticles by melt-emulsification, and to investigate their physicochemical characteristics.

MATERIALS AND METHODS

Reagents. The following materials were used as supplied without further purification: Soy bean lecithin (Phospholipon® 100, Nattermann, D-Köln); sodium glycocholate (Sigma, USA-St. Louis); tyloxapol (Eastman Kodak, USA-Kingsport); thiomersal (Synopharm, D-Barsbüttel); vitamin A-alcohol (Sigma, USA-St. Louis); vitamin K_3 (Fluka, CH-Buchs); 3-(trimethylsilyl)-propanesulfonic acid sodium salt (DSS), deuterium oxide for spectroscopy, phosphate buffer pH 6.88 (Merck, D-Darmstad); bidistilled water. Coenzyme Q_{10} was donated by Kabi Invent AB, S-Huddinge.

Preparation of coenzyme Q_{10} nanoparticle dispersions. Coenzyme Q_{10} is melted at approximately 70°C. If lecithin is used, it is dispersed in the melt by probe sonication (Soniprep 150, MSE, GB-Crawley) until the dispersion appears optically clear. The heated aqueous phase optionally con-

[1] Institute of Pharmaceutical Technology, Technical University of Braunschweig, Mendelssohnstr. 1, D-38106 Braunschweig, Federal Republic of Germany.

[2] Present address: Astra Arcus AB, Pharmaceutical Research and Development, S-151 85 Södertälje,

[3] To whom correspondence should be addressed.

0724-8741/95/0200-0201$07.50/0

taining water soluble surfactants is added to the melt. The dispersion is produced either by probe sonication for 60 min or by homogenization of the predispersed system in a thermostatized high pressure homogenizer (Microfluidizer M-110T, Microfluidics Corp., USA-Newton; Micron Lab 40, APV Gaulin, D-Lübeck) with the predispersion being accomplished by high speed vortexing (Ultra-Turrax, Janke & Kunkel, D-Staufen) or probe sonication (Soniprep 150, MSE, GB-Crawley) for approx. 2 min. In drug-loaded coenzyme Q_{10} dispersions, the drug is dissolved in the coenzyme Q_{10} melt. All preparations contain 0.01% Thiomersal as a preservative.

Particle size analysis. Particle size measurements on suspensions of the raw material were performed on a laser diffractometer (Mastersizer MS 20, Malvern Instruments GmbH, D-Herrsching). Samples were dispersed in demineralized water containing sodium glycocholate as a wetting agent and were stirred during measurements. Size distributions were calculated by the Malvern software program applying Fraunhofer diffraction theory.

Dynamic light scattering experiments on the nanoparticle dispersions were performed on a photon correlation spectrometer (Zetasizer 3, Malvern Instruments GmbH, D-Herrsching) at an angle of 90° as described previously (10). The presented data was obtained by the exponential sampling method (11). The logarithmic relative frequency distribution was converted to a linear scale and the mean particle size was calculated from the linear distribution by number.

Zetapotential. The electrophoretic mobility was determined by laser Doppler anemometry (Zetasizer 3, Malvern Instruments, D-Herrsching) in a thermostatized microelectrophoresis cell (AZ 4, Malvern Instruments, D-Herrsching) as described previously (8) using phosphate buffer pH 6.88, diluted 1:25 in bidistilled water, as electrolyte. Each value is the mean of five measurements.

Transmission electron microscopy of freeze-fractured specimen. Samples were freeze-fractured at 173 K in a freeze-fracturing equipment (BAF 400, Balzers AG, CH-Liechtenstein). Fast freezing was accomplished by slush into melting propane. Shadowing of the samples was performed with platinum/carbon (layer thickness: 2 nm) at 45° and with pure carbon at 90° for replica preparation. Replica were cleaned with a 1:1 (v/v) chloroform/ethanol mixture. Replica on uncoated grids were viewed with a transmission electron microscope (EM 300, Philips, D-Kassel).

Cryo-electron microscopy of frozen-hydrated specimens. A few microliter of the CoQ_{10} dispersions were placed on perforated carbon film coated grids and the excess liquid was removed by placing a piece of filter paper on the carbon film for about a second. The sample was then cryofixed by shooting into liquid ethane (Zeiss cryo-box with cryo-transfer) and transferred into an energy-filtered transmission-cryo-electron microscope (EM902, Zeiss, D-Oberkochen).

Differential scanning calorimetry. Measurements were performed on a differential scanning calorimeter (DSC-2C, Perkin Elmer, D-Überlingen) connected to a data processing unit (Data Station 3600, Perkin Elmer, D-Überlingen). Approximately 10 mg of sample were weighed into standard aluminum pans (Perkin Elmer, D-Überlingen). An empty pan was used as a reference. A calibration graph (enthalpy vs. concentration) was set up by weighing concentrations of 0.2 to 10.0% (w/w) coenzyme Q_{10} into standard pans and adding water to a weight of approximately 10 mg. The pans were accurately weighed after hermetically closing the caps. Samples were heated at a scan rate of 10 K/min from 293 K to 363 K.

Proton nuclear magnetic resonance (^1H NMR) spectroscopy. Samples were either prepared in or diluted with deuterium oxide (details are specified in the text). 3-(Trimethylsilyl)-propanesulfonic acid sodium salt (DSS) [δ = 0.00 ppm] dissolved in D_2O (36.14 mg DSS in 10 ml D_2O) was used as an internal reference for quantitative analysis and was added in 1:5 portions to the samples. ^1H NMR spectra were obtained on either a AM-300 or a WM-400 high resolution NMR spectrometer (Bruker, D-Rheinstetten) operating at 300 or 40 MHz, respectively. Spectra were run at ambient temperature unless otherwise stated. 90° pulse widths were used with a pulse repetition time of 14 s, which allowed complete relaxation of the system. The relaxation time T_1 was determined by the inversion recovery method to be 3.2 s for the trimethylsilyl signal of DSS. FID's were Fourier transformed without line broadening.

Synchrotron radiation X-ray diffraction. Measurements were performed on a double focussing monochromator mirror camera (12) in HASYLAB on the storage ring DORIS of the Deutsches Elektronen Synchrotron (DESY) as described previously (10).

RESULTS AND DISCUSSION

Preparation and particle size determination

The cardioprotective drug coenzyme Q_{10} (6-Decaprenyl-2,3-dimethoxy-5-methyl-1,4-benzoquinone) is a crystalline substance at room temperature. The orange coloured powder consists of crystal agglomerates in the size range of several microns up to the mm size range as determined by laser diffractometry and light microscopy of the raw material suspended in water containing sodium glycocholate as a wetting agent.

Aqueous dispersions with a CoQ_{10} content ranging from 1 to 10% (w/w) were prepared by emulsification of the molten substance in water employing various types and amounts of emulsifying agents. Emulsification was accomplished by probe sonication or high pressure homogenization. The emulsification efficiency of high pressure homogenization was higher than that of extensive probe sonication. As a result, the high pressure homogenized systems displayed a smaller mean particle size and a more narrow particle size distribution as presented in Fig. 1.

The composition of a selection of the prepared systems is summarized in Table I. All systems were prepared by high pressure homogenization.

The particle size distribution of the prepared systems was determined by photon correlation spectroscopy (PCS). Systems A, B, C and F displayed a narrow and monomodal size distribution in the lower nanometer range with the minimum and maximum PCS diameters ranging between approximately 40–50 nm and 190–210 nm. The PCS particle size distribution of system B is presented in Figure 1. Size

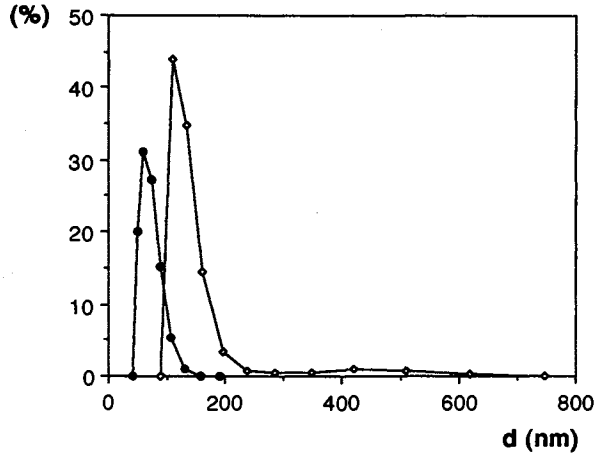

Fig. 1 Comparison of the particle size distribution by number (relative frequency vs. diameter) of similarly composed CoQ_{10} dispersions prepared by probe sonication (◇) and high pressure homogenization (●). (Composition: 3% CoQ_{10}, 1.8% PL, 0.4% SGC)

measurements by laser diffractometry suggest that the dispersions contain no particles >1 μm. Although the laser diffractometer is not suitable to determine the mean particle diameter of the systems since it fails to measure particles below about 100 nm, the instrument is sensitive to detect larger particles in the micrometer range.

Systems D and E were produced under moderate homogenization conditions and therefore display larger mean diameters. The examples demonstrate that the mean particle diameter of the CoQ_{10} dispersions can be varied within a considerable range by variations of the process parameters such as homogenization equipment, homogenization parameters (time, cycles, pressure), and the composition of the dispersions (type and amount of emulsifier, phase ratio). The observed effects are in accordance with results obtained on O/W emulsions (13).

Table I Composition, mean particle diameter and DSC results of selected CoQ_{10} nanoparticle dispersions

System[1]	Composition (w%)[2]	d (nm)	ΔH_T (J/g)
A	3% Q, 1.8% PL	103	0 (30)[3]
B	3% Q, 1.8% PL, 0.4% SGC	70	0 (30)
C	3% Q, 1.5% PL, 0.3% SGC	69	0 (30)
D	10% Q, 6% PL, 1.25% SGC	144	0 (21)
E	10% Q, 1.2% PL, 0.4% SGC	259	0 (21)
F	3% Q, 2% Tyl	67	0 (10)
G	3% Q, 1.8% PL, 0.4% SGC, 0.1% Vit. A	107	0 (10)
H	3% Q, 1.8% PL, 0.4% SGC, 0.1% Vit. K_3	102	0 (10)

Abbreviations: d = mean particle diameter determined by PCS (number distribution); ΔH_T = heat of transition determined by DSC; Q = coenzyme Q_{10}; PL = phospholipids; SGC = sodium glycocholate; Tyl = Tyloxapol; Vit. A = retinol alcohol; Vit. K_3 = menadione.

[1] Preparation:
Systems A-C: 10 min at 85 MPa (Microfluidizer M-110T)
Systems D, E: 5 cycles at 50 MPa (Micron Lab 40)
Systems F-H: 10 cycles at 120 MPa (Micron Lab 40)

[2] Difference to 100% is composed of bidistilled water.

[3] Values in brackets refer to the maximum time of storage after which the DSC measurements were performed.

The CoQ_{10} nanoparticle dispersions remain stable on storage at +4°C as judged from macroscopic observation and PCS measurements. No pronounced particle growth could be detected over the monitored period of up to 30 months.

The use of the nonionic surfactant tyloxapol (system F) yielded very homogenously sized particles with a smaller mean diameter than dispersions prepared by the use of phospholipids (system A). The mixture of phospholipids and bile salts (systems B and C) resulted in smaller particle sizes than lecithin alone. Reduction in mean particle diameter of approximately 30% resulting from the addition of sodium glycocholate could be observed. This reduction in diameter of 30% corresponds to a reduction in particle volume to a third and thus increases the number of particles per volume unit by factor 3. In order to exclude an influence of the increased total amount of emulsifier in system B compared to system A, system C was prepared with a reduced amount of phospholipid and bile salt at a constant molar ratio. As a result, the mean particle size of system C was still reduced compared to system A with the same total amount of emulsifier.

Glycocholate is a highly mobile ion and is thus supposed to support the emulsifying role of the comparingly slowly moving phospholipids by stabilizing the freshly generated surfaces during the homogenization process. The employed amount of bile salt was below the critical micelle concentration (cmc) of sodium glycocholate (cmc = 12 mmol = 5.9 g/l (14)) to provide for the immediate availability of glycocholate ions for surface stabilization. Zetapotential (ZP) measurements indicate that the glycocholate ion is associated with the phospholipid layer. The surface of the bile salt containing dispersions B (ZP = −40 mV) and C (ZP = −35 mV) is more negatively charged than that of system A (ZP = −28 mV).

CoQ_{10} nanoparticles can also serve as a carrier system for lipophilic drugs. Vitamins A (retinol alcohol) and K_3 (menadione) were incorporated as model drug substances (Table I, systems G and H). The drug-loaded dispersions remained stable on storage over the monitored period of 12 months. Precipitation of the model drugs could not be detected.

The observed stability of the CoQ_{10} dispersion emulsified by phospholipids only (system A) is different from observations obtained on tripalmitate and hard fat nanoparticles. The latter tend to gel forming ointment-like structures when stabilized by phospholipids only (8). This phenomenon seems to be related to the crystallization of the dispersed phase which is associated with an enormous increase of the surface area due to the formation of anisometric platelet-like particles (8). Gelation can, however, be prevented by the use of co-surfactants such as sodium glycocholate or tyloxapol. It is assumed that these co-surfactants serve as a reservoir of stabilizing agent which is immediately available as soon as recrystallization of the lipid takes place (15). The stability of system A, however, indicates that the physicochemical characteristics of CoQ_{10} nanoparticles are different from tripalmitate or hard fat dispersions. In order to elucidate the internal structure of CoQ_{10} particles, a study on the recrystallization tendency of the drug was performed on selected systems.

Characterization of selected systems

The structure of the CoQ_{10} nanoparticles was investigated by transmission electron microscopy (TEM) of freeze-fractured replica. TEM micrographs show spherical particles with an amorphous core (Fig. 2). The shape of the particles as well as the non-structured particle core point to the absence of a recrystallization of the drug since recrystallized particles tend to form anisometrical particle shapes and always display a structured particle core as was demonstrated for tripalmitate nanoparticles (8). The TEM results on the particle shape of CoQ_{10} nanoparticles could be verified by cryo-electron microscopy (Fig. 3). In addition, this method allows to detect phospholipid liposomes beside CoQ_{10} nanoparticles. The ring-shaped images of the vesicles can be distinguished from the disc-shaped images of the CoQ_{10} nanoparticles. The electron microscopic studies on high pressure homogenized dispersions indicate that the excess of phospholipids forms predominantly small unilamellar vesicles in the continuous phase as has been observed earlier for colloidal phospholipid-stabilized oil-in-water emulsions (16).

Both electron microscopic techniques give an idea of the obtained particle sizes. In the case of the cryo-electron microscopic studies, the low thickness of the ice films of the frozen-hydrated specimens in the holes of the perforated carbon film resulted in a non-random distribution of the particles with respect to particle size (Fig. 3) and impeded statistically relevant evaluations of the real particle size distribution. Fig. 3 demonstrates, however, that large numbers of extremely tiny CoQ_{10} nanoparticles with diameters below about 35 nm exist beside small unilamellar vesicles (SUVs) with diameters in the same size range. TEM pictures of freeze-fractured replica show the fractures of emulsion droplets and vesicle calottes only. Real particle diameters can be calculated from the diameters of fractures and calottes (17), but this is an extremely time-consuming analysis and requires artefact-free replica which are, however, rarely obtained. Even though a particle size analysis of TEM pictures was not performed since the number of imaged particles was too low, the direct inspection of the pictures of the fractured samples allows a rough estimate of the particle sizes. The TEM results support the cryo-electron microscopic observations concerning the particle diameters. There is also considerable agreement with PCS size results although the latter indicate higher diameters which is a consequence of PCS emphasizing larger particles due to the fact that the scattering intensity is related to the sixth power of the radius so that smaller particles might not be detected in the presence of larger ones (17).

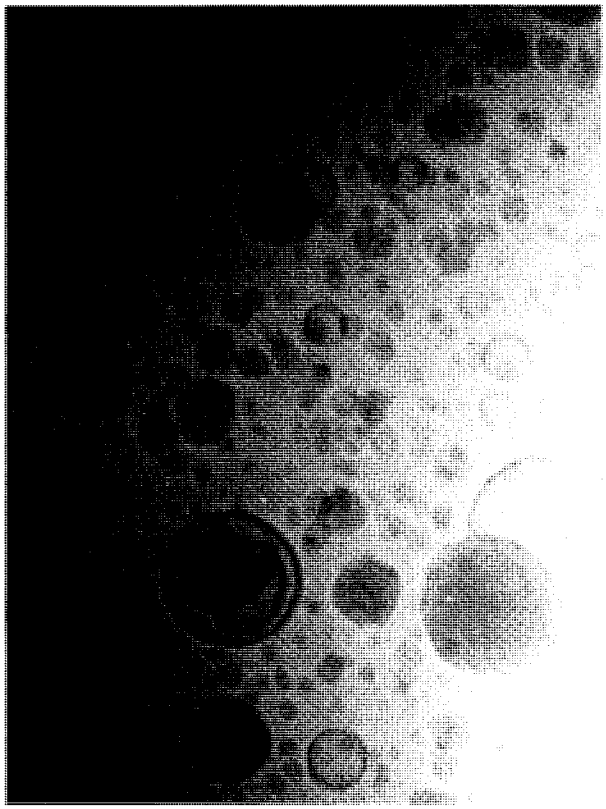

Fig. 3 Cryo-electron microscopic picture of a frozen-hydrated CoQ_{10} dispersion. The bar indicates 100 nm.

Fig. 2 Transmission electron micrograph of system B. The bar indicates 100 nm.

Further investigations on the physical state of the CoQ_{10} nanoparticles were performed by differential scanning calorimetry (DSC). All DSC thermograms recorded on the CoQ_{10} particle dispersions did not reveal any transition peak (first order phase transition) or glass transition (second order phase transition) in the range from room temperature to 80°C (Table I). Figure 4 represents the DSC thermograms of system A stored for 30 months at 4°C and of system E stored for 21 months at 4°C compared to a suspension of 3% crystalline CoQ_{10} in water which shows an endothermic transition peak with a maximum at 48°C corresponding to the melting of the substance. The slight baseline shift observed in all thermo-

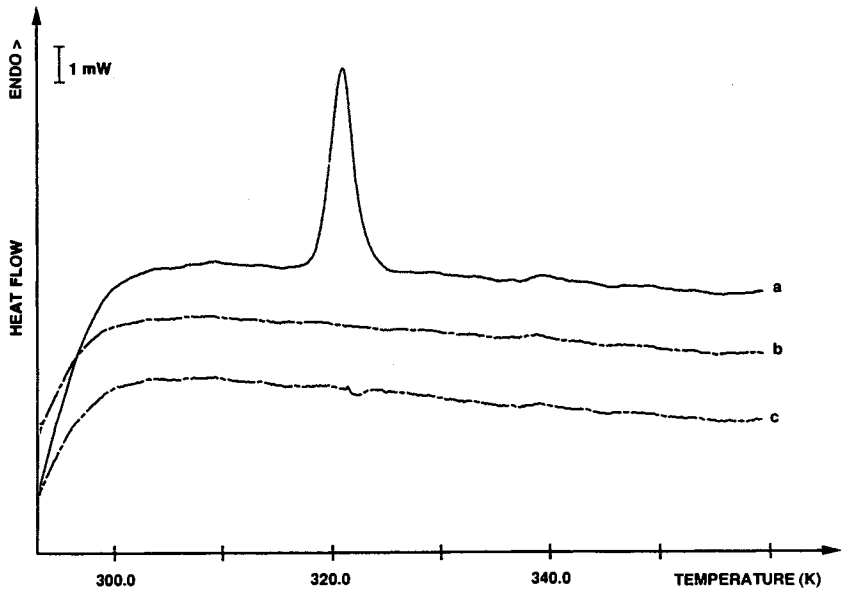

Fig. 4 DSC thermograms of a suspension of a) 3% crystalline CoQ_{10} in water, b) system A, and c) system E. Scan rate: 10 K/min.

grams at approximately 65°C, i.e. at a temperature above the melting point of CoQ_{10}, might be attributed to an impurity of the raw material and is currently under further investigation.

In order to exclude that the absence of transition peaks is related to the relatively low concentration of CoQ_{10} in the investigated systems, a calibration graph was set up recording DSC thermograms of differently concentrated suspensions of crystalline CoQ_{10} in water (concentration range: 0.2 to 10 w%). Concentrations of crystalline CoQ_{10} such small as 0.2% could still be detected by DSC suggesting that even if only 2% of the 10% CoQ_{10} dispersions (systems D and E) were crystalline a transition peak should have been observed.

Further evidence for the absence of drug recrystallization in the CoQ_{10} nanoparticle dispersions was obtained by X-ray diffraction studies. Crystalline CoQ_{10} exhibits two typical long spacings at 2.80 nm and 5.67 nm in the small angle region, and two sharp reflections at 0.395 nm and 0.49 nm in the wide angle region. For the CoQ_{10} dispersions, however, no diffraction peaks could be detected by small and wide angle X-ray diffraction using synchrotron radiation pointing to the conclusion that the drug is in a non-crystalline state (Fig. 5).

Although the investigations reported so far gave clear indications that the drug CoQ_{10} did not recrystallize after emulsification of the melt, the applied methods could not unambiguously answer the question whether the CoQ_{10} nanoparticles were in an amorphous solid or an amorphous liquid state. The absence of a glass transition in the DSC thermograms hinted at a liquid state of the finely dispersed CoQ_{10}.

Additional investigations on the physical state of the submicron-sized CoQ_{10} particles were performed by ^1H NMR spectroscopy. Due to differences in the mobility of hydrogen nuclei it is possible to distinguish between solid and liquid materials by this method (18). Spectra of a crude suspension of crystalline CoQ_{10} powder in deuterium oxide (D_2O) stabilized by sodium glycocholate were recorded at room temperature and after melting the CoQ_{10} substance. CoQ_{10} was suspended in D_2O in order to avoid disturbing signals from water. The obtained spectra revealed that the suspension of crystalline CoQ_{10} did not show any signals which could be assigned to the drug substance (Fig. 6b). The detected signals correspond to sodium glycocholate present in the D_2O phase (Fig. 6a). The spectrum recorded after heating of the crude dispersion to approximately 65°C for about 1 min (Fig. 6c), however, reveals signals at approximately 1.6 ppm, 2.0 ppm, 3.1 ppm, 3.8 ppm and 5.1 ppm which could be distinctly assigned to liquid CoQ_{10}. The observed line broadening of the peaks can be attributed to particle size and viscosity effects.

The aqueous CoQ_{10} nanoparticle dispersion of system B had to be diluted with 15% D_2O for ^1H NMR spectroscopy in order to locate the lock signal of the sample. The obtained spectrum (Fig. 7a) contains signals at 1.6 ppm, 2.0 ppm, 3.1 ppm and 3.8 ppm (chemical shift in ppm referred to TMS)

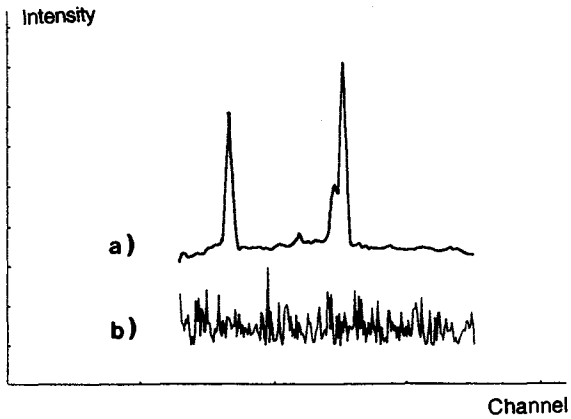

Fig. 5 Synchrotron radiation wide angle X-ray diffraction patterns of crystalline CoQ_{10} (above) and of system A (below). Exposure time: 3 min.

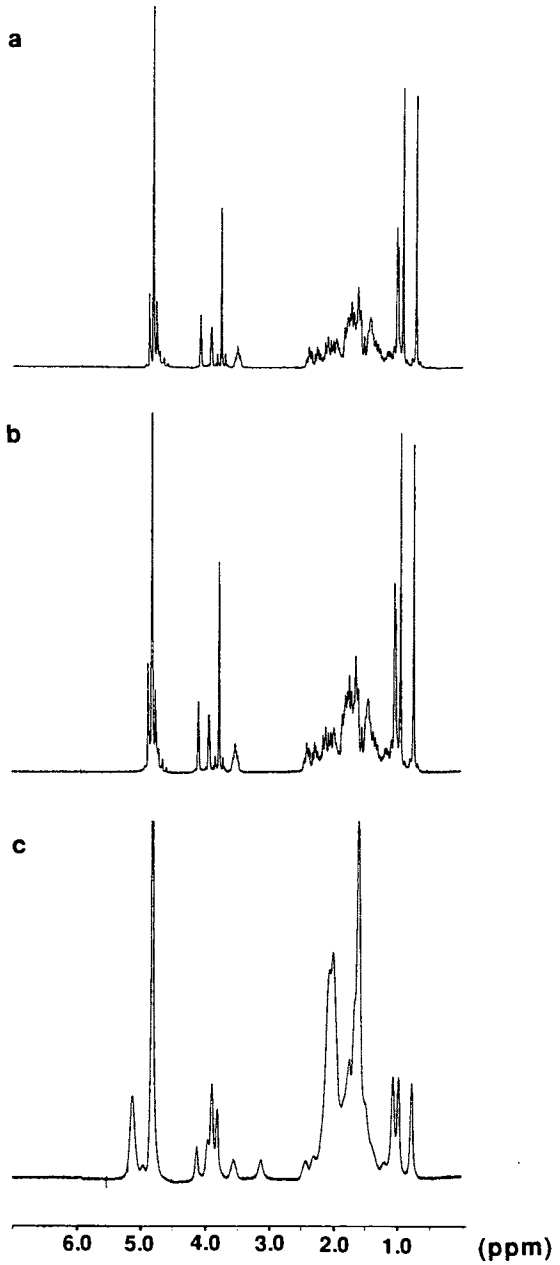

Fig. 6 ^{1}H-NMR spectra of a) a solution of sodium glycocholate in D_2O, b) crystalline CoQ_{10} suspended in a solution of sodium glycocholate in D_2O, and c) melted CoQ_{10} suspended in a solution of sodium glycocholate in D_2O.

which can be assigned to liquid (supercooled) CoQ_{10} hinting at the presence of drug which did not solidify. The signal at 5.1 ppm is superimposed by the huge water signal. In order to exclude disturbances from the water signal, a CoQ_{10} dispersion similarly composed as system B was prepared in D_2O by probe sonication. The deuterium oxide preparation exhibited an average particle size by number of about 144 nm in PCS experiments and displayed a broader particle size distribution than system B. The cryo-electron microscopic studies indicated that the preparation of the D_2O dispersion by probe sonication resulted in some structural changes compared with aqueous samples prepared by high pressure

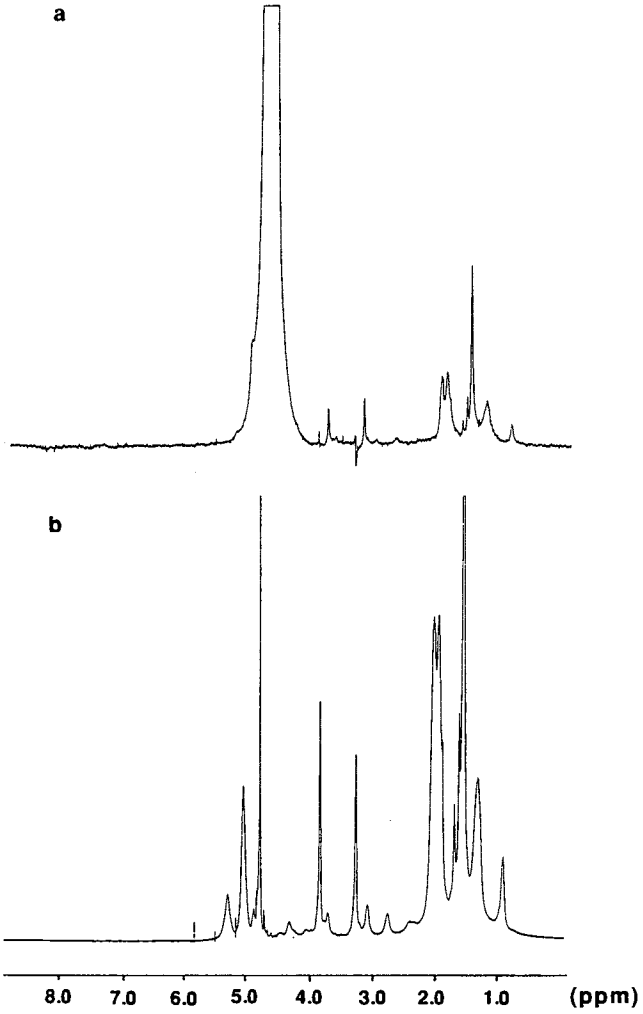

Fig. 7 ^{1}H-NMR spectra of a) system B diluted with 15% D_2O and b) a similarly composed dispersion prepared in D_2O by probe sonication.

homogenization. In the D_2O containing NMR sample, multilamellar phospholipid arrangements and some comparably huge CoQ_{10} nanoparticles could be observed. In the corresponding ^{1}H NMR spectrum (Fig. 7b) the signals at 1.6 ppm, 2.0 ppm, 3.1 ppm, 3.8 ppm and 5.1 ppm of liquid CoQ_{10} were better resolved than in system B diluted with 15% D_2O. The CoQ_{10} dispersion in D_2O was used for a (semi-)quantitative analysis of the liquid, i.e., supercooled CoQ_{10} in the colloidal dispersion. ^{1}H NMR spectra were taken from the deuterium oxide dispersion after storage of the sample for more than 20 months at 4°C. DSS (δ = 0.00 ppm) was added as an internal reference to the continuous phase. No relaxation regent was added. The area of the proton signal of the reference at 0.0 ppm was compared with the CoQ_{10} signal at 5.1 ppm which represents a strong signal since it corresponds to the (−CH = C) protons of the 10 isoprenoid units. The peak areas were calculated by weighing the corresponding paper areas. A computer-aided analysis of peak integrals was not possible due to imperfections in baseline and line-shape of the CoQ_{10} signal. The weight of CoQ_{10} (W_A) in the mixture with DSS (W_B) was derived from the following equation (19):

$$W_A = W_B \cdot N_B/N_A \cdot A_A/A_B \cdot M_A/M_B$$

where N indicates the number of signal protons, A the relative area of the signals and M the molecular weight of substance A (CoQ_{10}) or B (DSS). The signal area at 5.1 ppm corresponds to about 2.3% (w/w) CoQ_{10} indicating that most of the CoQ_{10} molecules in the comparably crude D_2O dispersion were still in a liquid state after more than 20 months of storage at 4°C.

DISCUSSION

The present study demonstrates that it is possible to prepare stable submicron-sized formulations of CoQ_{10} by emulsification of the molten substance in an aqueous phase using probe sonication or high pressure homogenization. The production avoids the use of organic solvents or any other potentially toxic excipients and employs physiologically acceptable compounds only. The manufacturing process can be accomplished by inexpensive, conventional techniques, and provides a product which is safe with respect to its handling. The process can potentially be employed for the production of small particles from low melting ($<\approx$95°C), poorly water soluble bioactive substances such as drugs, nutrient additives, herbicides, pesticides etc. A considerable number of compounds which meet these criteria can be found in the literature (e.g. 20).

In contrast to micronized powders which are often aerophilic due to the production process resulting in a poor wettability, the melt-emulsified drug particles exhibit hydrophilic surfaces. Moreover, the reduced particle size may enhance the apparent solubility of the compound according to the modified Gibbs-Kelvin equation (5):

$$\log \frac{S_r}{S_\infty} = \frac{2\gamma V}{2.303\ R\ T\ r}$$

where S_r is the solubility of a small particle of radius r, S_∞ that of an infinitively large one, γ is the interfacial energy, V the molar volume, R the gas constant and T the absolute temperature. It has been demonstrated before that the degree of absorption from the intestinum and the consequent blood levels of certain drugs are inversely related to particle size (21). Hence, the oral bioavailability of several drugs which are poorly soluble in the gastro-intestinal tract could be accelerated by a decrease in particle size.

Additionally, the reduction in size to the lower nanometer range would allow direct intravenous application of the water insoluble drug without the need of a carrier vehicle. Thus, possible problems such as drug leakage and physicochemical instability associated with the incorporation into a carrier could be circumvented. In addition, the very small particle size gives rise to a reduced uptake by the RES. Since RES activity is also influenced by surface characteristics, the drug nanoparticles may offer the possibility of a modified biodistribution by the modification of the particle surface which could be achieved by a proper choice of emulsifying agents. As the CoQ_{10} nanoparticles are in the size range of the endothelial fenestrations, they are potentially able to leave the vascular system to reach extravascular target sites.

The incorporation of the lipophilic model drugs retinol alcohol and menadione demonstrate that CoQ_{10} nanoparticles can be applied as an interesting alternative drug carrier system for poorly water soluble drugs. In contrast to parenteral emulsions containing vegetable oils such as soy bean oil as the dispersed phase, CoQ_{10} cannot be biodegraded by lipases. In addition, CoQ_{10} exhibits no measurable binding to serum proteins. As a consequence, the half life in blood of CoQ_{10} nanoparticles should be significantly higher than that of similarly sized droplets of vegetable oils stabilized by the same type of emulsifiers.

The physicochemical characterization of the prepared CoQ_{10} formulations revealed that the submiron-sized particles are of predominantly spherical shape and possess an amorphous core. Whereas TEM micrographs and X-ray diffraction patterns did not allow a clear distinction between amorphous solids and amorphous liquids, DSC and ^1H NMR data obtained on the submicron-sized CoQ_{10} dispersions indicate a liquid physical state of the particles. The results of the physicochemical characterization therefore suggest that the emulsified melt of CoQ_{10} does not recrystallize at temperatures of 4°C and above within the observation period. The CoQ_{10} nanoparticles thus represent a supercooled melt, and the formulations can be regarded as O/W emulsions according to the IUPAC definition (1). The degree of supercooling amounts to more than 45°C. The results can be partly explained by the colloidal size of the particles. Due to the increased Laplace pressure in the colloidal droplets of the dispersed CoQ_{10} melt, the chemical potential of the CoQ_{10} molecules is increased, i.e. they are in a higher energetic state than molecules in the bulk phase at a given temperature. Crystallization depends on the presence of nuclei of a critical size in which crystal growth can be continued. The rate of nucleation is determined by the probability of formation of critical-sized nuclei. This probability is reduced for molecules with a higher energy since nuclei of a size below the critical size can dissolve more easily if the molecules are in an elevated energetical state. As a consequence the temperature at which recrystallization starts is lower in dispersed colloidal droplets of the melt than in the bulk phase. Additionally, it should be considered that recrystallization has to start seperately in each single droplet.

Dispersed CoQ_{10} does not recrystallize in contrast to similarly prepared nanoparticles of glycerides such as tripalmitate and hard fat despite striking similarities in melting point of the bulk substances, composition of the dispersions, and their mean particle size (8,10). Although recrystallization of the glyceride nanoparticles requires a higher supercooling than the corresponding bulk materials, recrystallization of the dispersed lipids at 4°C or at room temperature is not prevented (22). In contrast, recrystallization of dispersed CoQ_{10} could not be observed over the monitored period of up to 30 months. The results indicate that crystallization in the dispersed state depends to a great extent on the properties of the matrix material, e.g. the crystal lattice. Obviously, the complexity of the CoQ_{10} crystal lattice does not permit the immediate crystallization of the molten substance at temperatures slightly below the melting point. The retarded formation of the CoQ_{10} crystal lattice is indicated by the high degree of supercooling of the bulk material. In DSC, recrystallization of bulk CoQ_{10} starts only at 7°C after melting and slow cooling (cooling rate: 1 K/min).

As a consequence of the liquid physical state of the submicron CoQ_{10} particles, their biopharmaceutical behav-

iour may be significantly different from that of the solid drug substance. Since the dissolution of liquid substances does not require crystal lattice energy, the peroral bioavailability of such nanoparticles is expected to be increased. Moreover, the colloidal size of the CoQ_{10} particles accounts for an apparent increase in the equilibrium solubility as predicted by the above mentioned Gibbs-Kelvin equation (5). An increase in peroral bioavailability can also be deduced from the increased dissolution rate as compared to conventional formulations owing to the colloidal particle size (increased interfacial area, decreased diffusional distance).

ACKNOWLEDGMENTS

The authors would like to thank Dr. V. Wray, C. Kakoschke and B. Jaschok-Kentner, National Research Center for Biotechnology, Braunschweig, Germany, for performance of the ^1H NMR experiments. We are indebted to Dr. M. H. J. Koch, European Molecular Biology Laboratory, Hamburg Outstion, DESY, Hamburg, Germany, for his assistance in the X-ray experiments. This work was financially supported by Kabi Invent AB, Huddinge, Sweden, and Pharmacia Oncology/Immunology, Helsingborg, Sweden.

REFERENCES

1. D. H. Everett. Report of the Commission on Colloid and Surface Chemistry of the Physical Chemistry Devision. *Pure Appl. Chem.* 31:577–638 (1972).
2. R. L. Juliano and D. Stamp. Effect of particle size and charge on the clearance rates of liposomes and liposome encapsulated drugs. *Biochim. Biophys. Res. Comm.* 63:651–658 (1975).
3. M. Bisrat, E. K. Anderberg, M. I. Barnett and C. Nyström. Physicochemical aspects of drug release. XV. Investigation of diffusional transport in dissolution of suspended, sparingly soluble drugs. *Int. J. Pharm.* 80:191–201 (1992).
4. A. T. Florence and D. Attwood. *Physicochemical Principles of Pharmacy,* Macmillan, London 1981.
5. G. Buckton and A. E. Beezer. The relationship between particle size and solubility. *Int. J. Pharm.* 82:R7–R10 (1992).
6. H. Kishi, N. Kanamori, S. Nishii, E. Hiraoka, T. Okamoto and T. Kishi. Metabolism of exogenous coenzyme Q_{10} in vivo and the bioavailability of coenzyme Q_{10} preparations in Japan. In: K. Folkers, Y. Yamamura (eds.), *Biomedical and Clinical Aspects of Coenzyme Q,* Vol. 4, Elsevier, Amsterdam, 1984, pp. 131–142.
7. C. Bogentoft, P. O. Edlund, B. Olsson, L. Widlund and K. Westesen. Biopharmaceutical aspects of intravenous and oral administration of coenzyme Q_{10}. In: K. Folkers, G. P. Littaru and T. Yamagami (eds.), *Biomedical and Clinical Aspects of Coenzyme Q,* Vol. 6, Elsevier, Amsterdam, 1991, pp. 215–224.
8. B. Siekmann and K. Westesen. Submicron-sized parenteral carrier systems based on solid lipids. *Pharm. Pharmacol. Lett.* 1:123–126 (1992).
9. T. Ramasarma. Lipid Quinones. In R. Paoletti and D. Kritchevski (eds.) *Adv. Lipid Res.,* Vol. 6, Academic Press, New York, 1968, pp. 107–180.
10. K. Westesen, B. Siekmann and M. H. J. Koch. Investigations on the physical state of lipid nanoparticles by synchrotron radiation X-ray diffraction. *Int. J. Pharm.* 93:189–199 (1993).
11. F. McNeil-Watson and A. Parker. Comparison of methods for high resolution sub-micron sizing by quasi-elastic light scattering (PCS). In: R. A. Williams, N. C. de Jaeger (eds.), *Advances in Measurement and Control of Colloidal Processes,* Butterworth-Heinemann Ltd., Oxford 1991, pp. 421–434.
12. M. H. J. Koch and J. Bordas. X-ray diffraction and scattering on disordered systems using synchrotron radiation. *Nucl. Instrum. Methods* 208:461–469 (1983).
13. P. Walstra. Formation of emulsions. In P. Becher (ed.), *Encyclopedia of Emulsion Technology,* Vol. 1, Marcel Dekker, New York, pp. 57–127.
14. A. Roda, A. F. Hofmann and K. J. Mysels. The influence of bile salt structure on self-association in aqueous solutions. *J. Biol. Chem.* 258:6362–6370 (1983).
15. K. Westesen and B. Siekmann. Comparison of parenteral lipid emulsions and solid lipid nanoparticles. *Eur. J. Pharm. Biopharm.* 40(Suppl.):35 S (1994).
16. K. Westesen and T. Wehler. Physicochemical Characterization of a Model Intravenous Emulsion. *J. Pharm. Sci.* 81:777–786 (1992).
17. K. Westesen and T. Wehler. Investigation of the Particle Size Distribution of a Model Intravenous Emulsion. *J. Pharm. Sci.* 82:1237–1244 (1993).
18. W. G. Proctor. An introduction to NMR. *J. Am. Oil Chem. Soc.* 48:1–3 (1971).
19. H. Günter. *NMR-Spektroskopie,* Thieme Verlag, Stuttgart, 1983.
20. Arzneibüro der ABDA. *Pharmazeutische Stoffliste* (*List of Pharmaceutical Substances*), 8th edn., Werbe- und Vertriebsgesellschaft Deutscher Apotheker, Frankfurt (Main), 1990.
21. R. M. Atkinson, C. Bedford, K. J. Child and E. G. Tomich. Effect of particle size on blood griseofulvin-levels in man. *Nature* 193:588–589 (1962).
22. B. Siekmann and K. Westesen. Thermoanalysis of the recrystallization process of melt-homogenized glyceride nanoparticles. *Colloids Surfaces B:* 3:159–175 (1994).